

Forecast the Principal, Stabilize the Residual: Subspace-Aware Feature Caching for Efficient Diffusion Transformers

Guantao Chen^{1,2} Shikang Zheng^{1,3} Yuqi Lin^{1,4} Linfeng Zhang^{1,†}

¹Shanghai Jiao Tong University

²Sun Yat-Sen University

³South China University of Technology

⁴Jilin University

Abstract

Diffusion Transformer (DiT) models have achieved unprecedented quality in image and video generation, yet their iterative sampling process remains computationally prohibitive. To accelerate inference, feature caching methods have emerged by reusing intermediate representations across timesteps. However, existing caching approaches treat all feature components uniformly. We reveal that DiT feature spaces contain distinct principal and residual subspaces with divergent temporal behavior: the principal subspace evolves smoothly and predictably, while the residual subspace exhibits volatile, low-energy oscillations that resist accurate prediction. Building on this insight, we propose SVD-*Cache*, a subspace-aware caching framework that decomposes diffusion features via Singular Value Decomposition (SVD), applies exponential moving average (EMA) prediction to the dominant low-rank components, and directly reuses the residual subspace. Extensive experiments demonstrate that SVD-*Cache* achieves near-lossless across diverse models and methods, including $5.55\times$ speedup on FLUX and HunyuanVideo, and compatibility with model acceleration techniques including distillation, quantization and sparse attention. Our code is in supplementary material and will be released on Github.

1. Introduction

Diffusion Transformer (DiT) models have demonstrated remarkable performance in both image and video generation, exhibiting powerful modeling capabilities and high-quality outputs, but their iterative denoising process incurs high computational cost. This substantial computational overhead poses challenges for deployment in latency-sensitive or resource-constrained environments, motivating ongoing efforts to develop more efficient inference techniques.

Two main acceleration strategies have emerged to address this: reducing the number of sampling steps through algorithmic innovations [20], and decreasing per-step computational cost via architectural improvements [37, 43]. Among these approaches, training-free feature caching stands out. By leveraging temporal coherence in hidden representations and reusing cached features, it significantly reduces computational redundancy. Pioneering work like DeepCache [23] validated this concept on U-Net models, subsequent methods including FORA [28], ToCa [48], and TaylorSeer [17] extended caching to transformer architectures and formulated feature caching as temporal evolution of hidden states. These approaches, however, implicitly assume that the entire feature space is smooth and predictable, thus applying a single prediction strategy can model the whole space. Yet, the feature space of diffusion transformers is extremely high-dimensional and expecting a globally smooth temporal trajectory across all dimensions may be untenable. This conjecture motivates us to dive into the potential subspaces of diffusion features and treat each subspace accordingly, rather than enforcing a one-size-fits-all predictor over the whole space.

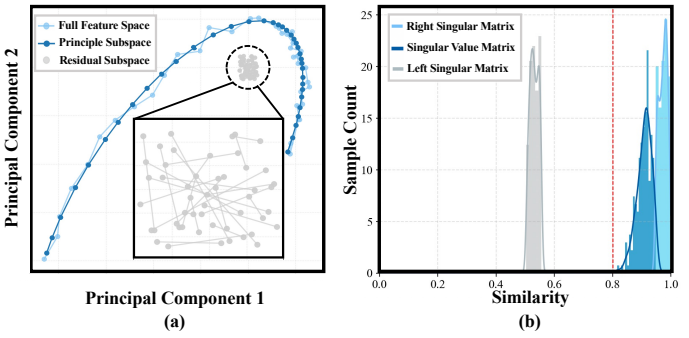


Figure 1. (a) PCA visualization of different feature spaces: Original Full Feature Subspace shows oscillatory trajectory while Principal Subspace evolves smoothly. Residual subspace is oscillatory and low-energy. (b) Singular values and right singular vectors are stable across different prompts. Similarity is evaluated using the product of cosine similarity and magnitude similarity. A similarity over 0.8 typically indicates a stable and reusable subspace.

We begin by visualizing the trajectory of the full feature

[†]Corresponding author.

space. As shown in Fig. 1(a), the trajectory is coherent yet noticeably oscillatory, confirming our intuition that global prediction is unreliable. We therefore decompose the feature space using singular value decomposition (SVD) into a rank- k principal subspace and an orthogonal residual subspace. The principal subspace, as illustrated in Fig. 1(a), evolves smoothly and predictably, thus supporting stable extrapolation. In contrast, the residual subspace displays high-frequency, low-energy fluctuations that are intrinsically hard to forecast and prone to error amplification. These observations argue for a nuanced, subspace-aware strategy: apply prediction where dynamics are stable (principal subspace) and simply reuse features where prediction is inherently unreliable (residual subspace).

Therefore, we propose **SVD-Cache**, a subspace-aware feature caching framework that decomposes DiT features via Singular Value Decomposition (SVD), applying distinct methods to different subspaces. SVD-Cache begins by decomposing the feature space to dominant and residual subspaces, and then applies EMA prediction to the dominant subspace while reusing the residual subspace directly. Intuitively, the decomposition needs to be performed across diverse prompts. However, we surprisingly uncover an intriguing property that for different prompts, the SVD decomposition yields **highly stable singular values and right singular matrices** as shown in Fig. 1(b), though the left singular matrices do not show such invariance, they can be reconstructed from the current features at low cost. This invariance allows us to decompose the feature space on a reference prompt offline and cost-effectively reconstruct the decomposition for any input prompt. Thus, with “*One-Time SVD*” performed offline for each model, “*All-Time Decomposition*” becomes possible with minimal additional cost.

SVD-Cache delivers robust, near-lossless accelerations across models and tasks. On FLUX and HunyuanVideo, it achieves $5.55 \times$ speedup with negligible quality drop. Moreover, it remains compatible with distillation, quantization and sparse-attention, with up to $29.01 \times$ speedup on FLUX.1-schnell, $7.61 \times$ speedup on FLUX.1-DEV-int8 and $10.73 \times$ with sparse-attention under minimal degradation. Our contributions are summarized as follows:

- **Subspace Heterogeneity.** We show that DiT features exhibit heterogeneous temporal dynamics across subspaces: the principal subspace evolves smoothly and predictably, while the residual is low-energy yet oscillatory and suitable for direct reuse. Through decomposition analyses across different prompts, we further reveal that the singular values and right singular matrices are input invariant.
- **SVD-Cache Framework.** Motivated by the observation that diffusion features evolve in a highly structured yet heterogeneous manner across different subspaces, we propose an SVD-based feature caching framework that partitions diffusion features into a rank- k principal subspace where

we apply EMA and a residual subspace directly reused.

- **Outstanding Results.** We validate SVD-Cache on multiple DiT models for both image and video generation, including FLUX and HunyuanVideo. Other acceleration models or methods such as FLUX.1-schnell, FLUX.1-Int8 and sparse attention were also evaluated. Our method consistently achieves state-of-the-art performance.

2. Related Work

Diffusion models [8, 30] have demonstrated remarkable capabilities in image and video generation. While early implementations commonly relied on U-Net architectures [25], their scalability constraints were later mitigated by Diffusion Transformers (DiT) [24], which enabled significant improvements in quality and resolution across multiple modalities [2, 3, 36, 46]. Despite these advances, the core limitation of diffusion models remains their iterative sampling process, which introduces substantial computational overhead during inference. This has motivated two key research directions: minimizing the number of sampling steps, and reducing the per-step computational cost. Beyond raw efficiency, an ongoing challenge lies in preserving generative fidelity and stability, particularly under aggressive acceleration.

2.1. Sampling Timestep Reduction

A major approach to acceleration involves reducing the number of diffusion steps. DDIM [31] first introduced a deterministic sampling strategy that allows fast generation without compromising perceptual quality. Subsequently, higher-order solvers such as DPM-Solver and its variants [20, 21, 44] have achieved better trade-offs between accuracy and efficiency by employing advanced numerical discretization schemes with controlled local truncation error. Other methods like Rectified Flow [18] shorten transport trajectories in latent space, while progressive distillation [27] compresses long diffusion chains into compact generative models. More recently, consistency models [32] have enabled direct few-step synthesis by learning a noise-to-signal mapping in a consistent framework.

2.2. Denoising Network Acceleration

A wide range of model compression techniques aim to reduce the cost of each denoising step. These include structural pruning [6, 47], low-bit quantization [11, 14, 29], knowledge distillation [15], and token-level reduction strategies [1, 5, 10, 38, 39]. Although these methods are effective in decreasing inference latency and memory usage, they often require additional retraining and may suffer performance degradation under distributional shifts.

Feature caching is an orthogonal acceleration paradigm that reduces redundant computation by reusing intermediate activations across timesteps. Early efforts in U-Net-style models [13, 23] have evolved into DiT-specific designs,

including FasterCache [22], FORA [28], Δ -DiT [4], Tea-Cache [16]. These approaches vary in cache granularity and update frequency. Recent developments further extend this line of work through dynamic update schemes (e.g., ToCa, DuCa) [48, 49], unified cache-prune frameworks [33], and region-aware sampling [19]. Notably, TaylorSeer [17] exemplifies the *cache-then-forecast* paradigm, leveraging polynomial extrapolation over cached feature sequences to anticipate future activations with minimal overhead.

3. Method

3.1. Preliminary

Diffusion Models. Diffusion models generate data by simulating a forward-reverse stochastic process. The forward process gradually corrupts a data sample x_0 with Gaussian noise:

$$x_t = \sqrt{\alpha_t} x_0 + \sqrt{1 - \alpha_t} \epsilon_t, \quad \epsilon_t \sim \mathcal{N}(0, \mathbf{I}), \quad (1)$$

where α_t is a decreasing noise schedule. After T steps, the sample approaches pure noise. The reverse process learns to recover x_0 by predicting the noise component $\epsilon_\theta(x_t, t)$, commonly parameterized as:

$$x_{t-1} = \frac{1}{\sqrt{\alpha_t}} \left(x_t - \frac{1 - \alpha_t}{\sqrt{1 - \bar{\alpha}_t}} \epsilon_\theta(x_t, t) \right) + \sigma_t \epsilon, \quad (2)$$

where $\bar{\alpha}_t = \prod_{s=1}^t \alpha_s$, and σ_t controls residual noise.

Feature Caching. Feature caching seeks to accelerate diffusion sampling by reusing intermediate activations across timesteps, thus avoiding redundant computation. At timestep t , the network produces hidden feature maps $\mathcal{F}_t = \{\mathcal{F}_t^l\}_{l=1}^L$. A caching function $\mathcal{C}(\mathcal{F}_A, k)$ estimates the feature $\tilde{\mathcal{F}}_k$ at a future timestep k based on previously cached representations:

$$\tilde{\mathcal{F}}_k = \mathcal{C}(\mathcal{F}_t, k) := \mathcal{F}_t, \quad \forall k \in (t, t + n - 1]. \quad (3)$$

This reuse strategy provides an approximate $(n-1) \times$ reduction in computation. Recent methods enhance this paradigm by forecasting future features rather than directly copying them.

3.2. Low-Rank Approximation via SVD

Let $F \in \mathbb{R}^{N \times D}$ denote the feature matrix for a chosen DiT block. We compute a singular value decomposition (SVD):

$$F = U \Sigma V^\top \quad U \in \mathbb{R}^{N \times r}, \quad \Sigma \in \mathbb{R}^{r \times r}, \quad V \in \mathbb{R}^{D \times r} \quad (4)$$

where $r = \text{rank}(F)$ and singular values in Σ are sorted in descending order. We retain the top- k components ($k \ll r$) to form a rank- k approximation:

$$F_k = U_k \Sigma_k V_k^\top. \quad (5)$$

Rank selection. We determine k using an energy threshold τ based on the cumulative singular value energy:

$$\frac{\sum_{i=1}^k \sigma_i^2}{\sum_{i=1}^r \sigma_i^2} \geq \tau, \quad (6)$$

where $\{\sigma_i\}$ are singular values of F_t . This adaptive criterion preserves most of the representational energy while discarding redundant or noisy dimensions.

3.3. One-Time SVD and Basis Reuse

As observed in Fig. 1(b), both the singular values σ and the right singular matrix V exhibit minimal variation across different input prompts, which allows us to reuse these components for efficient low-rank subspace reconstruction.

Reference Basis Caching. We first perform SVD on the feature space of a reference prompt and store its essential components for reuse. Specifically, we cache the right singular matrix V_C and the singular value vector σ_C :

$$\text{cache : } V_C \in \mathbb{R}^{D \times r}, \quad \sigma_C = [\sigma_1, \dots, \sigma_r]^\top \in \mathbb{R}^r. \quad (7)$$

Low-Rank Subspace Reconstruction. For any subsequent prompt with feature space F , we reuse the cached basis to reconstruct its low-rank subspace without recomputing SVD. The left singular matrix is approximated as:

$$U = F V_C \text{ diag}(\sigma_C)^{-1} \quad (8)$$

Then, the rank- k approximation of F is obtained by truncating the components:

$$F_k = U_k \text{ diag}(\sigma_{C,k}) V_{C,k}^\top \quad (9)$$

where U_k , $\sigma_{C,k}$, and $V_{C,k}$ denote the top- k components of U , σ_C , and V_C , respectively.

Finally, the residual component is computed as:

$$R = F - F_k \quad (10)$$

3.4. Exponential Moving Average for Prediction

Exponential moving average (EMA) is a lightweight temporal forecasting method that assigns exponentially decaying weights to past observations. In our setting, we use EMA to predict the future low-rank features $\{F_{k,t}\}$ based on their stable temporal evolution across denoising steps.

EMA Formulation. Let $F_{k,t}$ denote the rank- k feature representation at caching timestep t . We maintain an EMA state $\hat{F}_{k,t}$, which is recursively updated as:

$$\hat{F}_{k,t} = \beta \hat{F}_{k,t-\Delta} + (1 - \beta) F_{k,t}, \quad (11)$$

where $\beta \in (0, 1)$ controls the trade-off between smoothness and responsiveness: larger β yields smoother long-range predictions, while smaller β reacts more quickly to short-term changes in $F_{k,t}$. The updated EMA state $\hat{F}_{k,t}$ is then used to predict the next cached timestep, approximating $F_{k,t+\Delta}$. Practically, we set $\beta = 0.9$ in all experiments.

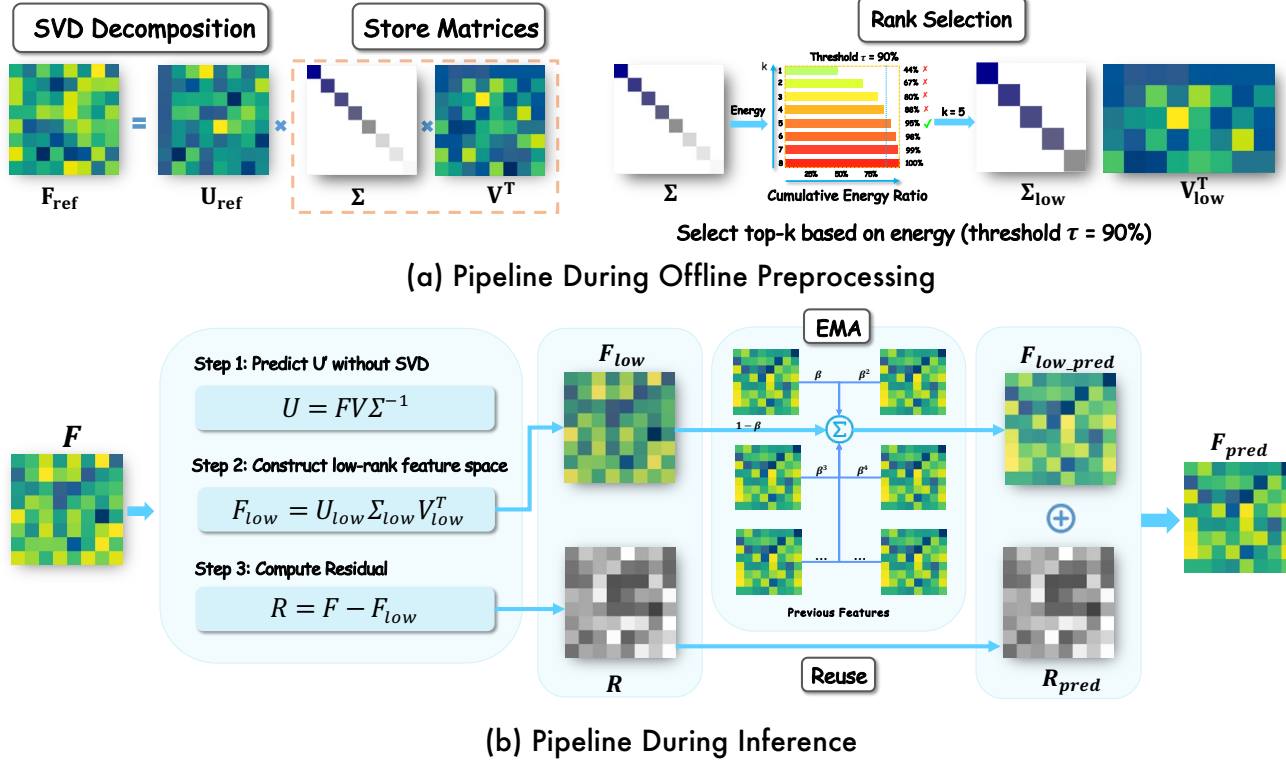


Figure 2. Overview of the proposed SVD-Cache framework. At each diffusion timestep, we decompose the feature map into principal and residual subspaces via SVD. The principal subspace, which captures the most significant variations and evolves smoothly, is predicted using exponential moving average (EMA). The residual subspace, containing high-frequency details that resist accurate prediction, is directly reused. This hybrid strategy allows us to efficiently cache features while maintaining high fidelity in the generated outputs.

3.5. SVD-Cache Framework

SVD-Cache establishes a shared low-rank basis by performing one-time SVD on a reference prompt. The resulting right singular vectors V_C and singular values σ_C are cached following Eq. (7), forming a universal subspace that can be reused across prompts. Given a new prompt with feature matrix F , we reconstruct its low-rank representation in this cached subspace. The feature is projected onto the reference basis to obtain approximate left singular vectors using Eq. (8), which are then truncated to produce the rank- k approximation F_k as in Eq. (9). The orthogonal residual R is computed through Eq. (10); it captures the high-frequency, low-energy components that lie outside the principal subspace.

We then treat the subspaces respectively. The low-rank feature F_k , which exhibits smooth and stable temporal evolution, is predicted using an EMA-based forecaster, yielding the next-step approximation $\hat{F}_{k,t+\Delta}$. The residual, in contrast, shows much weaker temporal coherence and is difficult to forecast reliably (as illustrated in Fig. 1(a)). To prevent error amplification, we simply reuse it across timesteps: $\hat{R}_{t+\Delta} = R_t$. The final feature at the future timestep is reconstructed by combining the EMA-predicted low-rank feature

with the reused residual: $\hat{F}_{t+\Delta} = \hat{F}_{k,t+\Delta} + \hat{R}_{t+\Delta}$.

This hybrid design leverages the predictability of principal directions while safely reusing the high-frequency residual, enabling SVD-Cache to maintain accuracy and stability at significantly reduced computational cost.

4. Experiments

4.1. Experiment Settings

Model Configurations. We evaluate two representative diffusion models—FLUX.1-dev [12] for text-to-image and HunyuanVideo [34] for text-to-video—and further test compatibility with FLUX.1-dev-torchao-int8 (quantization), FLUX.1-schnell (step distillation), and sparse-attention variants. This setup verifies that our method integrates seamlessly with quantization, distillation, and sparse-attention-based acceleration techniques.

Evaluation and Metrics. For text-to-image tasks, we follow DrawBench [26], reporting ImageReward [35], CLIP Score [7], and PSNR/SSIM/LPIPS. For text-to-video generation, we evaluate HunyuanVideo using VBench [9], which measures motion, appearance, and semantic consistency.

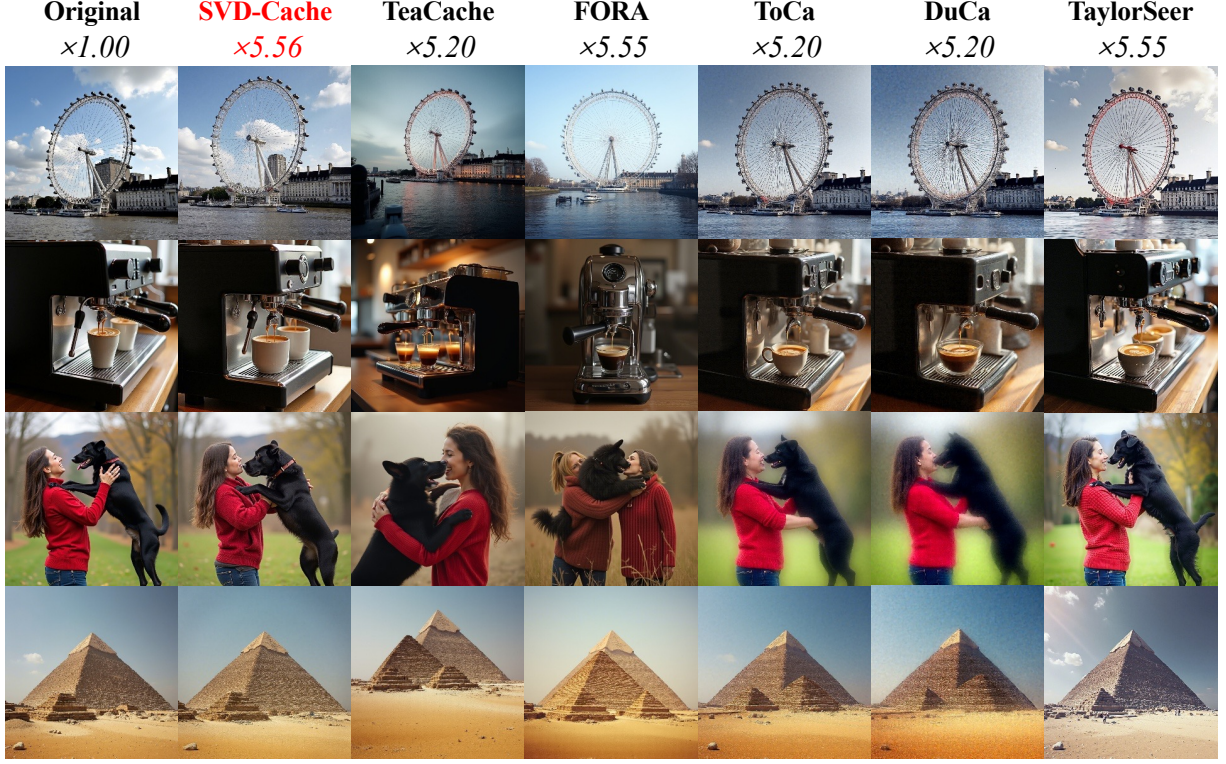


Figure 3. Visual Comparison of $5.5 \times$ accelerated FLUX between different feature cache methods.

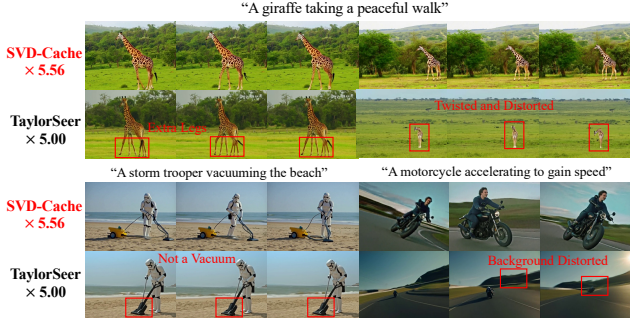


Figure 4. Comparison between SVD-Cache and TaylorSeer on HunyuanVideo. SVD-Cache sustains stronger temporal consistency and visual quality under more aggressive acceleration, while TaylorSeer develops visible artifacts and flickering.

4.2. Results on Text-to-Image Generation

As shown in Table 1, SVD-Cache consistently outperforms all baselines across acceleration levels on FLUX.1-dev. At interval $\mathcal{N} = 5$, it attains the best ImageReward (**1.0123**) and CLIP (**32.983**) with a $4.16 \times$ FLOPs reduction, surpassing reuse-based methods and prediction-based approaches such as TaylorSeer (0.9768 at $4.16 \times$) and FoCa (0.9713 at $4.99 \times$). At $\mathcal{N} = 6$, it remains competitive, achieving **1.0057** ImageReward and **33.027** CLIP at $5.00 \times$, outperforming

TaylorSeer and Speca under similar cost. Even under aggressive compression, SVD-Cache remains robust: at $\mathcal{N} = 7$, it delivers **0.9938** ImageReward with $5.55 \times$ FLOPs (vs. TaylorSeer 0.9698, FoCa 0.9713); and at $\mathcal{N} = 8$, it still maintains strong quality (ImageReward **0.9769**, CLIP **32.848**) with a $6.24 \times$ speedup. These results highlight SVD-Cache’s superior efficiency–quality trade-off across a broad range of compression regimes.

4.3. Results on Text-to-Video Generation.

We evaluate SVD-Cache on HunyuanVideo and compare it with recent acceleration baselines. As shown in Table 2, SVD-Cache achieves state-of-the-art performance across all acceleration settings. At $\mathcal{N} = 5$, it reaches a VBench score of **80.60**, nearly matching the original model (80.66) while reducing FLOPs by **5.00 \times** , outperforming TaylorSeer (79.93), Speca (79.98), and FoCa (79.96) at similar cost. At $\mathcal{N} = 6$, it achieves the fastest latency (**29.77s**) and a **5.56 \times** FLOPs reduction, while maintaining a strong VBench score of **80.46**. This surpasses robust baselines such as DuCa (78.72) and ToCa (78.86), demonstrating superior stability under aggressive skipping. Overall, these results confirm the robustness of SVD-Cache for video generation.

Table 1. Quantitative comparison of text-to-image generation on FLUX.1-dev.

Method	Efficient Attention	Acceleration				Image Reward \uparrow	CLIP Score \uparrow
		Latency(s) \downarrow	Speed \uparrow	FLOPs(T) \downarrow	Speed \uparrow		
FLUX.1							
[dev]: 50 steps	✓	25.82	1.00 \times	3719.50	1.00 \times	0.9898 (+0.000%)	32.404 (+0.000%)
60% steps	✓	16.70	1.55 \times	2231.70	1.67 \times	0.9663 (-2.371%)	32.312 (-0.283%)
Δ -DiT ($\mathcal{N} = 2$)	✓	17.80	1.45 \times	2480.01	1.50 \times	0.9444 (-4.594%)	32.273 (-0.404%)
Δ -DiT ($\mathcal{N} = 3$)	✓	13.02	1.98 \times	1686.76	2.21 \times	0.8721 (-11.90%)	32.102 (-0.933%)
TaylorSeer ($\mathcal{N} = 3, O = 2$)	✓	9.89	2.61 \times	1320.07	2.82 \times	0.9989 (+0.919%)	32.413 (+0.027%)
FoCa ($\mathcal{N} = 3$)	✓	9.28	2.78 \times	1327.21	2.80 \times	0.9890 (-0.081%)	32.577 (+0.533%)
SVD-Cache ($\mathcal{N} = 4$)	✓	8.09	3.19\times	967.91	3.84\times	1.0147 (+2.519%)	32.840 (+1.348%)
34% steps	✓	9.07	2.85 \times	1264.63	3.13 \times	0.9453 (-4.498%)	32.114 (-0.893%)
Chipmunk	✓	12.72	2.02 \times	1505.87	2.47 \times	0.9936 (+0.384%)	32.548 (+0.444%)
FORA ($\mathcal{N} = 3$)	✓	10.16	2.54 \times	1320.07	2.82 \times	0.9776 (-1.232%)	32.266 (-0.425%)
ToCa ($\mathcal{N} = 6$)	✗	13.16	1.96 \times	924.30	4.02 \times	0.9802 (-0.968%)	32.083 (-0.990%)
DuCa ($\mathcal{N} = 5$)	✓	8.18	3.15 \times	978.76	3.80 \times	0.9955 (+0.576%)	32.241 (-0.503%)
TaylorSeer ($\mathcal{N} = 4, O = 2$)	✓	9.24	2.80 \times	967.91	3.84 \times	0.9857 (-0.414%)	32.413 (+0.027%)
FoCa ($\mathcal{N} = 4$)	✓	9.35	2.76 \times	1050.70	3.54 \times	0.9757 (-1.424%)	32.538 (+0.414%)
Clusca ($\mathcal{N} = 4, O = 2, K = 16$)	✓	9.25	2.79 \times	1045.58	3.56 \times	0.9850 (-0.485%)	32.441 (+0.114%)
SVD-Cache ($\mathcal{N} = 5$)	✓	7.62	3.38\times	893.54	4.16\times	1.0123 (+2.267%)	32.983 (+1.788%)
FORA ($\mathcal{N} = 4$)	✓	8.12	3.14 \times	967.91	3.84 \times	0.9730 (-1.695%)	32.142 (-0.809%)
ToCa ($\mathcal{N} = 8$)	✗	11.36	2.27 \times	784.54	4.74 \times	0.9451 (-4.514%)	31.993 (-1.271%)
DuCa ($\mathcal{N} = 7$)	✓	6.74	3.83\times	760.14	4.89 \times	0.9757 (-1.424%)	32.066 (-1.046%)
TeaCache ($l = 0.8$)	✓	7.21	3.58 \times	892.35	4.17 \times	0.8683 (-12.28%)	31.704 (-2.159%)
TaylorSeer ($\mathcal{N} = 5, O = 2$)	✓	7.46	3.46 \times	893.54	4.16 \times	0.9768 (-1.314%)	32.467 (+0.194%)
FoCa ($\mathcal{N} = 6$)	✓	7.54	3.42 \times	745.39	4.99 \times	0.9713 (-1.870%)	32.922 (+1.600%)
Speca ($\mathcal{N}_{\max} = 8, \mathcal{N}_{\min} = 2$)	✓	7.42	3.48 \times	791.38	4.70 \times	0.9985 (+0.878%)	32.277 (-0.391%)
Clusca ($\mathcal{N} = 5, O = 1, K = 16$)	✓	7.05	3.66 \times	897.03	4.14 \times	0.9718 (-1.818%)	32.319 (-0.262%)
SVD-Cache ($\mathcal{N} = 6$)	✓	6.81	3.79 \times	744.81	5.00\times	1.0057 (+1.605%)	33.027 (+1.921%)
FORA ($\mathcal{N} = 6$)	✓	8.17	3.16 \times	744.80	4.99 \times	0.7760 (+21.62%)	31.742 (-2.043%)
ToCa ($\mathcal{N} = 10$)	✗	7.93	3.25 \times	714.66	5.20 \times	0.7155 (+27.70%)	31.808 (-1.839%)
DuCa ($\mathcal{N} = 9$)	✓	7.27	3.55 \times	690.25	5.39 \times	0.8382 (-15.33%)	31.759 (-1.993%)
TeaCache ($l = 1$)	✓	8.19	3.19 \times	743.63	5.01 \times	0.8379 (-15.36%)	31.877 (-1.627%)
TaylorSeer ($\mathcal{N} = 7, O = 2$)	✓	6.77	3.81 \times	671.39	5.54 \times	0.9698 (-2.020%)	32.128 (-0.851%)
Clusca ($\mathcal{N} = 6, O = 1, K = 16$)	✓	7.13	3.62 \times	748.48	4.97 \times	0.9704 (-1.956%)	32.217 (-0.577%)
SVD-Cache ($\mathcal{N} = 7$)	✓	6.43	4.01 \times	670.44	5.55 \times	0.9938 (+0.404%)	33.144 (+2.282%)
SVD-Cache ($\mathcal{N} = 8$)	✓	4.99	5.17\times	596.07	6.24\times	0.9769 (-1.306%)	32.848 (+1.369%)

4.4. Results on Acceleration Methods.

To assess generality, we apply SVD-Cache to several accelerated diffusion models and methods: the INT8-quantized FLUX.1-dev-int8, the step-distilled FLUX.1-schnell and sparse attention. As summarized in Table 3, SVD-Cache consistently provides significant speedup while maintaining or improving quality. Visual examples are shown in Fig. 6.

On FLUX.1-dev-int8, SVD-Cache ($\mathcal{N} = 5$) reaches an ImageReward of **0.9904** and CLIP **32.88**, and surpasses the original quantized baseline (1.0160) on PSNR (29.74), SSIM (0.708), and LPIPS (0.3214). On the distilled FLUX.1-schnell (NFE = 4, 8), it offers flexible trade-offs—for example, at $\mathcal{N} = 3$, it delivers a $49.87\times$ FLOPs reduction with an ImageReward of **0.9463**, outperforming TaylorSeer and TeaCache under the same NFE.

SVD-Cache is orthogonal to quantization, distillation,

and sparse attention, operating purely at inference through feature reuse and solver scheduling. It integrates seamlessly with existing compression methods, enabling additive speedups without retraining or reparameterization.

4.5. Ablation Study.

Ablation study is conducted on FLUX. We first investigate the impact of applying different methods on the low-rank subspace and the residual component separately. As shown in Fig 5(c), applying EMA prediction on the low-rank subspace while reusing the residual yields the best performance, validating our design choice. Using direct reuse for both components leads to significant quality degradation, while applying EMA to both results in error accumulation.

We also conduct an ablation study to investigate how different choices of the energy threshold τ (Eq(6)) affect the decomposition. As shown in Fig. 5(d), we find that the

Table 2. Quantitative comparison of text-to-video generation on HunyuanVideo.

Method HunyuanVideo	Efficient Attention	Acceleration				VBench \uparrow Score(%)
		Latency(s) \downarrow	Speed \uparrow	FLOPs(T) \downarrow	Speed \uparrow	
Original: 50 steps	✓	145.00	1.00 \times	29773.0	1.00 \times	80.66 (+0.0%)
22% steps	✓	31.87	4.55 \times	6550.1	4.55 \times	78.74 (-2.4%)
AdaCache	✓	55.34	2.62 \times	11192.8	2.66 \times	80.12 (-0.7%)
TeaCache ($l = 0.4$)	✓	30.49	4.76 \times	6550.1	4.55 \times	79.36 (-1.6%)
FORA ($\mathcal{N} = 6$)	✓	34.39	4.22 \times	5960.4	5.00 \times	78.83 (-2.3%)
ToCa ($\mathcal{N} = 5, R = 90\%$)	✗	38.52	3.76 \times	7006.2	4.25 \times	78.86 (-2.2%)
DuCa ($\mathcal{N} = 5, R = 90\%$)	✓	31.69	4.58 \times	6483.2	4.48 \times	78.72 (-2.4%)
TaylorSeer ($\mathcal{N} = 5, O = 1$)	✓	34.84	4.16 \times	5960.4	5.00 \times	79.93 (-0.9%)
Speca ($\mathcal{N}_{\max} = 8, \mathcal{N}_{\min} = 2$)	✓	34.58	4.19 \times	5692.7	5.23 \times	79.98 (-0.8%)
Clusca ($\mathcal{N} = 5, O = 1, K = 16$)	✓	35.37	4.10 \times	5373.0	5.54 \times	79.96 (-0.9%)
FoCa ($\mathcal{N} = 5$)	✓	34.52	4.20 \times	5966.5	4.99 \times	79.96 (-0.8%)
SVD-Cache ($\mathcal{N} = 5$)	✓	34.69	4.18 \times	5960.4	5.00 \times	80.60 (-0.1%)
SVD-Cache ($\mathcal{N} = 6$)	✓	29.77	4.87\times	5359.1	5.56\times	80.46 (-0.2%)

Table 3. Quantitative comparison of other accelerated models on FLUX.

Method	NFE	Acceleration				Quality Metrics		Perceptual Metrics		
		Latency(s) \downarrow	Speed \uparrow	FLOPs(T) \downarrow	Speed \uparrow	ImageReward \uparrow	CLIP \uparrow	PSNR \uparrow	SSIM \uparrow	LPIPS \downarrow
FLUX.1[dev]	50	25.82	1.00 \times	3719.50	1.00 \times	0.9898	32.40	-	-	-
FLUX.1[dev]-int8	50	13.17	1.96 \times	1823.30	2.04 \times	1.0160	32.60	∞	1.000	0.000
SVD-Cache ($\mathcal{N} = 5$)	50	3.39	7.61 \times	438.29	8.49 \times	0.9904	32.88	29.74	0.708	0.3214
FLUX[SparsAttention]	50	7.36	3.51 \times	979.50	3.80 \times	0.8358	32.49	∞	1.000	0.000
SVD-Cache ($\mathcal{N} = 5$)	50	2.40	10.73 \times	318.45	11.68 \times	0.8177	32.48	30.02	0.808	0.254
FLUX[schnell]	8	4.21	6.14 \times	595.12	6.25 \times	0.9090	33.93	∞	1.000	0.000
SVD-Cache ($\mathcal{N} = 2$)	8	2.85	9.06 \times	372.15	9.99 \times	0.9285	33.92	34.81	0.936	0.047
SVD-Cache ($\mathcal{N} = 5$)	8	1.69	15.22\times	223.20	16.66\times	0.9713	34.68	30.01	0.745	0.272
FLUX[schnell]	4	2.34	11.03 \times	297.60	12.50 \times	0.9129	34.15	∞	1.000	0.000
TaylorSeer ($\mathcal{N} = 2$)	4	1.58	16.34 \times	209.70	17.74 \times	0.9012	33.76	29.13	0.746	0.249
TeaCache ($l = 0.6$)	4	1.26	20.49 \times	163.78	22.71 \times	0.8921	33.87	28.01	0.379	0.734
SVD-Cache ($\mathcal{N} = 2$)	4	1.16	22.25 \times	152.32	24.42 \times	0.9247	34.20	34.83	0.947	0.037
SVD-Cache ($\mathcal{N} = 3$)	4	0.89	29.01\times	74.58	49.87\times	0.9463	34.65	29.70	0.785	0.176

- The PSNR, SSIM, and LPIPS of SVD-Cache are computed with respect to the outputs of the corresponding accelerated baselines instead of the original model. SparsAttention[40] [41] [42] is a universal training-free sparse attention accelerating language, image, and video models.

optimal energy threshold is around 0.85. Setting τ higher leads to an overly large low-rank subspace that absorbs high-frequency noise, reducing prediction stability and degrading EMA accuracy. Conversely, choosing a smaller τ makes the low-rank subspace too restrictive, discarding essential structural components and causing noticeable errors.

5. Discussion

5.1. Why Feature Space Decomposition?

Prior caching methods implicitly assume that all feature dimensions evolve smoothly over time, which is rarely true in high-dimensional hidden states. Only a part of feature space shows stable, predictable dynamics based on our observation; the remaining contains high-frequency fluctuations that are difficult to forecast and easily amplify prediction errors.

Operating directly in the full space therefore mixes stable and unstable directions, leading to rapid error growth.

By decomposing features, SVD-Cache predicts only the smooth, low-rank component where forecasting is reliable, while handling the volatile residual conservatively through reuse or mild smoothing. This selective treatment makes caching both more stable and accurate. As shown in Fig. 5(a), this decomposition consistently outperforms variants that attempt to predict the full feature space.

5.2. Compatibility with Acceleration Methods.

SVD-Cache follows a central principle of diffusion acceleration: **preserve essential structure** while down-weighting components with limited influence. By decomposing features into a dominant subspace and an orthogonal residual,

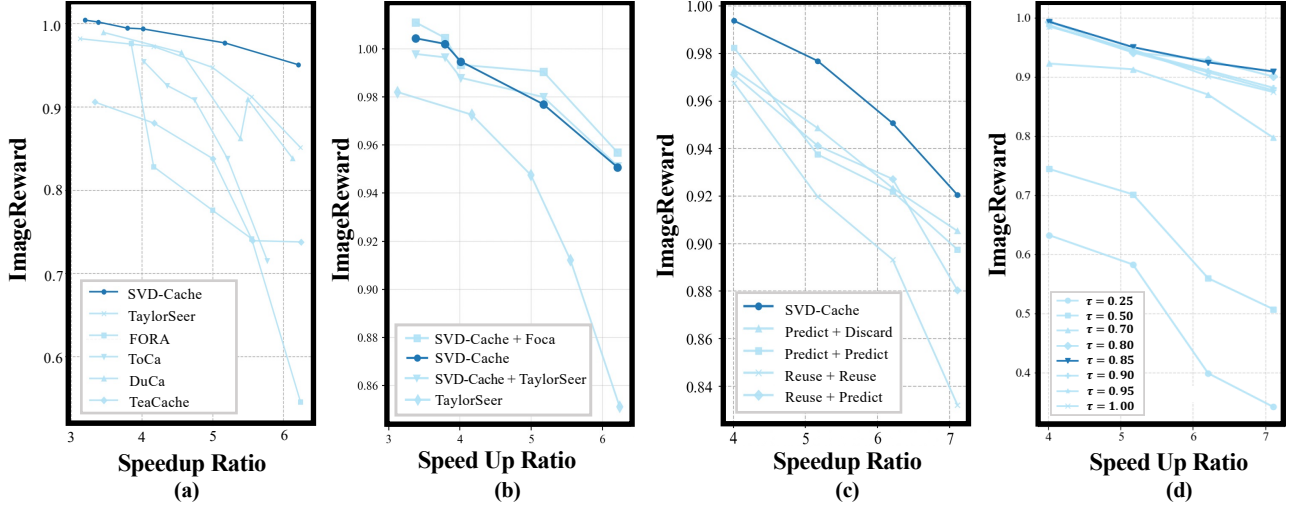


Figure 5. **Overall and Ablation Results of SVD-Cache.** (a) SVD-Cache consistently outperforms token-wise(ToCa) and other full-feature-space predictor baselines. (b) When the low-rank subspace is predicted with other ODE methods, quality is significantly improved over the original method. (c) Ablation study on Flux by applying different strategies to the low-rank and residual components separately. (d) Ablation study on the energy threshold τ for subspace decomposition.



Figure 6. Images of SVD-Cache applied on different accelerated diffusion models.

it forecasts only the stable, high-utility directions and handles the volatile tail conservatively—naturally aligning with major acceleration families.

Distilled models benefit because SVD-Cache avoids extrapolating along unstable, high-curvature directions where full-space predictors often fail. Quantized models gain from prediction in a compressed coordinate system that attenuates quantization noise, with the residual reused rather than aggressively forecasted. Sparse-attention methods benefit similarly, as SVD-Cache emphasizes principal structure in feature space. Together, subspace-restricted forecasting, residual stabilization, and one-time basis reuse provide robustness and low overhead, integrating cleanly with step-skipping or lightweight sampling schedules.

5.3. Compatibility with Other Caching Methods

SVD-Cache is orthogonal to existing caching methods such as TaylorSeer [17] and FoCa [45], which focus on designing better predictors over the entire feature space. In contrast, SVD-Cache introduces a subspace-aware strategy that decomposes the feature space and applies different caching strategies to each subspace. Therefore, SVD-Cache can be integrated with these methods by replacing their full-space predictors with our subspace-aware design, yielding further gains in caching efficiency and quality preservation, as shown in Fig. 5(b). When paired with TaylorSeer, SVD-Cache delivers substantial improvements over the TaylorSeer, and its combination with more recent approaches such as FoCa demonstrates even more promising results.

6. Conclusion

We presented SVD-Cache, a training-free feature caching framework for diffusion transformers that leverages low-rank feature decomposition and stable subspace prediction to reduce computation while preserving generation quality. Through a one-time SVD and dimension-wise residual modeling, SVD-Cache provides robust, scalable caching across prompts and timesteps. Extensive experiments on images and videos demonstrate consistent state-of-the-art performance across a wide range of acceleration ratios, outperforming existing reuse and forecast-based methods. Moreover, SVD-Cache is orthogonal to quantization, distillation, and sparse attention, enabling additive speedups without retraining and providing a practical path toward scalable, plug-and-play acceleration for modern diffusion models.

References

- [1] Daniel Bolya and Judy Hoffman. Token merging for fast stable diffusion. In *Proceedings of the IEEE/CVF conference on computer vision and pattern recognition*, pages 4599–4603, 2023. [2](#)
- [2] Junsong Chen, Chongjian Ge, Enze Xie, Yue Wu, Lewei Yao, Xiaozhe Ren, Zhongdao Wang, Ping Luo, Huchuan Lu, and Zhenguo Li. Pixart- σ : Weak-to-strong training of diffusion transformer for 4k text-to-image generation, 2024. [2](#)
- [3] Junsong Chen, Jincheng Yu, Chongjian Ge, Lewei Yao, Enze Xie, Yue Wu, Zhongdao Wang, James Kwok, Ping Luo, Huchuan Lu, and Zhenguo Li. Pixart- α : Fast training of diffusion transformer for photorealistic text-to-image synthesis. In *International Conference on Learning Representations*, 2024. [2](#)
- [4] Pengtao Chen, Mingzhu Shen, Peng Ye, Jianjian Cao, Chongjun Tu, Christos-Savvas Bouganis, Yiren Zhao, and Tao Chen. δ -dit: A training-free acceleration method tailored for diffusion transformers. *arXiv preprint arXiv:2406.01125*, 2024. [3](#)
- [5] Xinle Cheng, Zhuoming Chen, and Zhihao Jia. Cat pruning: Cluster-aware token pruning for text-to-image diffusion models, 2025. [2](#)
- [6] Gongfan Fang, Xinyin Ma, and Xinchao Wang. Structural pruning for diffusion models. *arXiv preprint arXiv:2305.10924*, 2023. [2](#)
- [7] Jack Hessel, Ari Holtzman, Maxwell Forbes, Ronan Le Bras, and Yejin Choi. Clipscore: A reference-free evaluation metric for image captioning. *arXiv preprint arXiv:2104.08718*, 2021. [4](#)
- [8] Jonathan Ho, Ajay Jain, and Pieter Abbeel. Denoising diffusion probabilistic models. *Advances in neural information processing systems*, 33:6840–6851, 2020. [2](#)
- [9] Ziqi Huang, Yinan He, Jiashuo Yu, Fan Zhang, Chenyang Si, Yuming Jiang, Yuanhan Zhang, Tianxing Wu, Qingyang Jin, Nattapol Chanpaisit, Yaohui Wang, Xinyuan Chen, Limin Wang, Dahua Lin, Yu Qiao, and Ziwei Liu. VBench: Comprehensive Benchmark Suite for Video Generative Models, 2023. *arXiv:2311.17982 [cs]*. [4](#)
- [10] Minchul Kim, Shangqian Gao, Yen-Chang Hsu, Yilin Shen, and Hongxia Jin. Token fusion: Bridging the gap between token pruning and token merging. In *Proceedings of the IEEE/CVF Winter Conference on Applications of Computer Vision*, pages 1383–1392, 2024. [2](#)
- [11] Sungbin Kim, Hyunwuk Lee, Wonho Cho, Mincheol Park, and Won Woo Ro. Ditto: Accelerating diffusion model via temporal value similarity. In *Proceedings of the 2025 IEEE International Symposium on High-Performance Computer Architecture (HPCA)*. IEEE, 2025. [2](#)
- [12] Black Forest Labs. Flux. <https://github.com/black-forest-labs/flux>, 2024. [4](#)
- [13] Senmao Li, Taihang Hu, Fahad Shahbaz Khan, Linxuan Li, Shiqi Yang, Yaxing Wang, Ming-Ming Cheng, and Jian Yang. Faster diffusion: Rethinking the role of unet encoder in diffusion models. *arXiv preprint arXiv:2312.09608*, 2023. [2](#)
- [14] Xiuyu Li, Yijiang Liu, Long Lian, Huanrui Yang, Zhen Dong, Daniel Kang, Shanghang Zhang, and Kurt Keutzer. Q- diffusion: Quantizing diffusion models. In *2023 IEEE/CVF International Conference on Computer Vision (ICCV)*, pages 17489–17499, 2023. [2](#)
- [15] Yanyu Li, Huan Wang, Qing Jin, Ju Hu, Pavlo Chemerys, Yun Fu, Yanzhi Wang, Sergey Tulyakov, and Jian Ren. Snapfusion: Text-to-image diffusion model on mobile devices within two seconds. *Advances in Neural Information Processing Systems*, 36, 2024. [2](#)
- [16] Feng Liu, Shiwei Zhang, Xiaofeng Wang, Yujie Wei, Haonan Qiu, Yuzhong Zhao, Yingya Zhang, Qixiang Ye, and Fang Wan. Timestep embedding tells: It's time to cache for video diffusion model, 2024. [3](#)
- [17] Jiacheng Liu, Chang Zou, Yuanhuiyi Lyu, Junjie Chen, and Linfeng Zhang. From reusing to forecasting: Accelerating diffusion models with taylorseers, 2025. [1, 3, 8](#)
- [18] Xingchao Liu, Chengyue Gong, et al. Flow straight and fast: Learning to generate and transfer data with rectified flow. In *The Eleventh International Conference on Learning Representations*, 2023. [2](#)
- [19] Ziming Liu, Yifan Yang, Chengruidong Zhang, Yiqi Zhang, Lili Qiu, Yang You, and Yuqing Yang. Region-adaptive sampling for diffusion transformers, 2025. [3](#)
- [20] Cheng Lu, Yuhao Zhou, Fan Bao, Jianfei Chen, Chongxuan Li, and Jun Zhu. Dpm-solver: A fast ode solver for diffusion probabilistic model sampling in around 10 steps. *Advances in Neural Information Processing Systems*, 35:5775–5787, 2022. [1, 2](#)
- [21] Cheng Lu, Yuhao Zhou, Fan Bao, Jianfei Chen, Chongxuan Li, and Jun Zhu. Dpm-solver++: Fast solver for guided sampling of diffusion probabilistic models. *arXiv preprint arXiv:2211.01095*, 2022. [2](#)
- [22] Zhengyao Lv, Chenyang Si, Junhao Song, Zhenyu Yang, Yu Qiao, Ziwei Liu, and Kwan-Yee K. Wong. Fastercache: Training-free video diffusion model acceleration with high quality, 2025. [3](#)
- [23] Xinyin Ma, Gongfan Fang, and Xinchao Wang. Deepcache: Accelerating diffusion models for free. In *Proceedings of the IEEE/CVF Conference on Computer Vision and Pattern Recognition*, pages 15762–15772, 2024. [1, 2](#)
- [24] William Peebles and Saining Xie. Scalable diffusion models with transformers. In *Proceedings of the IEEE/CVF International Conference on Computer Vision*, pages 4195–4205, 2023. [2](#)
- [25] Olaf Ronneberger, Philipp Fischer, and Thomas Brox. U-net: Convolutional networks for biomedical image segmentation. In *Medical image computing and computer-assisted intervention–MICCAI 2015: 18th international conference, Munich, Germany, October 5–9, 2015, proceedings, part III* 18, pages 234–241. Springer, 2015. [2](#)
- [26] Chitwan Saharia, William Chan, Saurabh Saxena, Lala Li, Jay Wang, Karim Ghasemipour, Raphael Gontijo Lopes, Burcu Lee, Ekin Gontijo Lopes, Jonathan He, and et al. Photorealistic text-to-image diffusion models with deep language understanding. In *NeurIPS*, 2022. [4](#)
- [27] Tim Salimans and Jonathan Ho. Progressive distillation for fast sampling of diffusion models. *arXiv preprint arXiv:2202.00512*, 2022. [2](#)

[28] Pratheba Selvaraju, Tianyu Ding, Tianyi Chen, Ilya Zharkov, and Luming Liang. Fora: Fast-forward caching in diffusion transformer acceleration. *arXiv preprint arXiv:2407.01425*, 2024. 1, 3

[29] Yuzhang Shang, Zhihang Yuan, Bin Xie, Bingzhe Wu, and Yan Yan. Post-training quantization on diffusion models. In *Proceedings of the IEEE/CVF conference on computer vision and pattern recognition*, pages 1972–1981, 2023. 2

[30] Jascha Sohl-Dickstein, Eric Weiss, Niru Maheswaranathan, and Surya Ganguli. Deep unsupervised learning using nonequilibrium thermodynamics. In *International conference on machine learning*, pages 2256–2265. PMLR, 2015. 2

[31] Jiaming Song, Chenlin Meng, and Stefano Ermon. Denoising diffusion implicit models. In *International Conference on Learning Representations*, 2021. 2

[32] Yang Song, Prafulla Dhariwal, Mark Chen, and Ilya Sutskever. Consistency models. In *International Conference on Machine Learning*, pages 32211–32252. PMLR, 2023. 2

[33] Wenzhang Sun, Qirui Hou, Donglin Di, Jiahui Yang, Yongjia Ma, and Jianxun Cui. Unicp: A unified caching and pruning framework for efficient video generation, 2025. 3

[34] Xingwu Sun, Yanfeng Chen, Huang, et al. Hunyuan-large: An open-source MoE model with 52 billion activated parameters by tencent. 4

[35] Jiazheng Xu, Xiao Li, Guoli Xu, Yuan Zhang, Xinyu Zhang, Qishuo Zhou, Yanan Wang, Qiming Liu, Yunjie Zhang, Yuqing He, et al. Imagereward: Learning and evaluating human preferences for text-to-image generation. *arXiv preprint arXiv:2304.05977*, 2023. 4

[36] Zhuoyi Yang, Jiayan Teng, Wendi Zheng, Ming Ding, Shiyu Huang, Jiazheng Xu, Yuanming Yang, Wenyi Hong, Xiaohan Zhang, Guanyu Feng, Da Yin, Xiaotao Gu, Yuxuan Zhang, Weihan Wang, Yean Cheng, Bin Xu, Yuxiao Dong, and Jie Tang. Cogvideox: Text-to-video diffusion models with an expert transformer. In *The Thirteenth International Conference on Learning Representations*, 2025. 2

[37] Zhihang Yuan, Hanling Zhang, Pu Lu, Xuefei Ning, Linfeng Zhang, Tianchen Zhao, Shengen Yan, Guohao Dai, and Yu Wang. Diffastattn: Attention compression for diffusion transformer models. *arXiv preprint arXiv:2406.08552*, 2024. 1

[38] Evelyn Zhang, Bang Xiao, Jiayi Tang, Qianli Ma, Chang Zou, Xuefei Ning, Xuming Hu, and Linfeng Zhang. Token pruning for caching better: 9 times acceleration on stable diffusion for free, 2024. 2

[39] Evelyn Zhang, Jiayi Tang, Xuefei Ning, and Linfeng Zhang. Training-free and hardware-friendly acceleration for diffusion models via similarity-based token pruning. In *Proceedings of the AAAI Conference on Artificial Intelligence*, 2025. 2

[40] Jintao Zhang, Haofeng Huang, Pengle Zhang, Jia Wei, Jun Zhu, and Jianfei Chen. Sageattention2: Efficient attention with thorough outlier smoothing and per-thread int4 quantization. In *International Conference on Machine Learning (ICML)*, 2025. 7

[41] Jintao Zhang, Jia Wei, Pengle Zhang, Jun Zhu, and Jianfei Chen. Sageattention: Accurate 8-bit attention for plug-and-play inference acceleration. In *International Conference on Learning Representations (ICLR)*, 2025. 7

[42] Jintao Zhang, Chendong Xiang, Haofeng Huang, Jia Wei, Haocheng Xi, Jun Zhu, and Jianfei Chen. Spargeattn: Accurate sparse attention accelerating any model inference. In *International Conference on Machine Learning (ICML)*, 2025. 7

[43] Xuanlei Zhao, Xiaolong Jin, Kai Wang, and Yang You. Real-time video generation with pyramid attention broadcast. *arXiv preprint arXiv:2408.12588*, 2024. 1

[44] Kaiwen Zheng, Cheng Lu, Jianfei Chen, and Jun Zhu. DPM-solver-v3: Improved diffusion ODE solver with empirical model statistics. In *Thirty-seventh Conference on Neural Information Processing Systems*, 2023. 2

[45] Shikang Zheng, Liang Feng, Xinyu Wang, Qinming Zhou, Peiliang Cai, Chang Zou, Jiacheng Liu, Yuqi Lin, Junjie Chen, Yue Ma, and Linfeng Zhang. Forecast then calibrate: Feature caching as ode for efficient diffusion transformers, 2025. 8

[46] Zangwei Zheng, Xiangyu Peng, Tianji Yang, Chenhui Shen, Shenggui Li, Hongxin Liu, Yukun Zhou, Tianyi Li, and Yang You. Open-sora: Democratizing efficient video production for all, 2024. 2

[47] Haowei Zhu, Dehua Tang, Ji Liu, Mingjie Lu, Jintu Zheng, Jinzhang Peng, Dong Li, Yu Wang, Fan Jiang, Lu Tian, Sapan dan Tiwari, Ashish Sirasao, Jun-Hai Yong, Bin Wang, and Emad Barsoum. Dip-go: A diffusion pruner via few-step gradient optimization, 2024. 2

[48] Chang Zou, Xuyang Liu, Ting Liu, Siteng Huang, and Linfeng Zhang. Accelerating diffusion transformers with token-wise feature caching. *arXiv preprint arXiv:2410.05317*, 2024. 1, 3

[49] Chang Zou, Evelyn Zhang, Runlin Guo, Haohang Xu, Conghui He, Xuming Hu, and Linfeng Zhang. Accelerating diffusion transformers with dual feature caching, 2024. 3